Volume 49 Number 2 FEBRUARY 2009 ISSN 0890-6955

ELSEVIER

INTERNATIONAL JOURNAL OF

MACHINE TOOLS & MANUFACTURE

DESIGN, RESEARCH AND APPLICATION

Editor-in-Chief: T A Dean

Contents of this issue:

Continued on outside back cover

Available online at

ScienceDirect

www.sciencedirect.com

International Journal of Machine Tools & Manufacture 49 (2009) 134–141

Contents lists available at ScienceDirect

International Journal of Machine Tools & Manufacture

journal homepage: www.elsevier.com/locate/ijmactool

Abrasive waterjet peening with elastic prestress: A parametric evaluation

B. Sadasivam [a], A. Hizal [a], D. Arola [a,b,*]

[a] Department of Mechanical Engineering, University of Maryland Baltimore County, 1000 Hilltop Circle, Baltimore, MD 21250, USA
[b] Department of Endodontics, Prosthodontics and Operative Dentistry, Baltimore College of Dental Surgery, University of Maryland Baltimore, Baltimore, MD 21201, USA

ARTICLE INFO

Article history:
Received 29 July 2008
Received in revised form
24 September 2008
Accepted 8 October 2008
Available online 22 October 2008

Keywords:
Abrasive waterjet peening
Elastic prestress
Residual stress
Surface treatment

ABSTRACT

Abrasive waterjet peening (AWJP) has emerged as a potentially viable method of surface treatment for metal orthopedic devices. In this study the influences of AWJP with elastic prestress on the surface and subsurface residual stress distributions and surface texture of spring steel (ASTM 228) as well as titanium (Ti6Al4V) and nickel (inconel 718) alloys were studied. A design of experiments (DOE) and an analysis of variance (ANOVA) were used to identify the parameters with primary contributions to the dependent variables. Surface residual stress resulting from AWJP ranged from 500 to 2500 MPa, and the depth of compressive residual stress ranged from nearly 80 to 600 μm. While the elastic prestress had no effect on the surface texture, it was a primary contributor to the magnitude of surface residual stress, which increased with an increase in the elastic prestress. According to the results of this study, AWJP with elastic prestress can serve as a viable method of surface treatment in situations that require an increase in surface roughness and a compressive residual stress.

1. Introduction

Abrasive waterjet peening (AWJP) has emerged as a new surface treatment technique for engineering and biomedical components that is capable of introducing a rough surface texture without causing a substantial reduction in the fatigue strength [1–3]. The technique utilizes a high-pressure waterjet laden with abrasive particles to provide the kinetic energy necessary to achieve a combination of material removal and near-surface deformation of the target. Previous work has shown that AWJP is capable of introducing compressive residual stresses and with magnitude necessary to mitigate the potentially detrimental aspects of the surface texture on the fatigue behavior. In fact, in an application of AWJP to AISI 304 and Ti6Al4V targets the apparent endurance strength was increased up to 25% with respect to the wrought form metal, and despite a substantial increase in the surface roughness [3]. As such, AWJP may serve as an attractive surface treatment for applications where component functionality requires a high surface roughness and subsequent control or moderate improvements in the fatigue strength.

One evident drawback of AWJP is that the magnitude of residual stress is lower than that resulting from competitive processes like shot peening. For example, in AWJP of Ti6Al4V, the near-surface compressive residual stress ranged from 90 to 350 MPa [1], whereas shot peening of the same alloy was reported to result in a maximum residual stress of 700 MPa [4]. Similarly, AWJP of AISI 304 steel resulted in a maximum surface residual stress of 460 MPa [3], whereas shot peening of comparable alloys resulted in surface stresses between 650 [5] and 900 MPa [6]. Commercial applications of AWJP may be more likely if the process could be further improved by increasing the magnitude of compressive residual stress, thereby increasing the apparent fatigue strength.

In shot peening operations an elastic prestress has been applied to the target to increase the magnitude and depth of residual stress [7,8]. Briefly, the treatments are conducted while subjecting the target surface to a tensile elastic prestress. Upon releasing the prestress after treatment it superposes with the surface residual stress caused by peening and results in a higher compressive residual stress. Although application of elastic prestress has been shown to increase the magnitude of compressive residual stress in shot peening, this method has not been applied universally. In fact, the use of prestress (or prestrain) has received surprisingly little attention. Recent preliminary studies have shown that an elastic prestress can be used for increasing the magnitude and depth of residual stress in AWJP [9–11]. While promising, the parametric effects of elastic prestress on the surface and subsurface residual stress distribution resulting from AWJP remain unknown.

A design of experiments (DOE) approach has been widely used for evaluating the parametric effects of treatment parameters in manufacturing operations. In shot peening, a DOE has been used

* Corresponding author at: Department of Mechanical Engineering, University of Maryland Baltimore County, 1000 Hilltop Circle, Baltimore, MD 21250, USA.
Tel.: +1 410 455 3310; fax: +1 410 455 1052.
E-mail address: darola@umbc.edu (D. Arola).

0890-6955/$ - see front matter © 2008 Elsevier Ltd. All rights reserved.
doi:10.1016/j.ijmachtools.2008.10.001

to evaluate the parametric effects on the fatigue life and residual stress [12–14]. Specifically, Freddi et al. [12] evaluated the parametric effects of Almen intensity and shot diameter on the magnitude of compressive residual stress and fatigue life in treatment of nitriding steel. Parametric trends were identified for a depth of 25 μm from the treated surface and showed that the shot diameter was the most important parameter to the subsurface residual stress [12]. Similarly, George et al. [14] evaluated the effect of standoff distance, shot size, shot flow rate and peening time on the peening of grade II Almen strips using Taguchi techniques. Results showed that the standoff distance contributed to nearly 80% of the variation in peening intensity resulting from shot peening over the range in treatment conditions. Note that the aforementioned studies have been limited to evaluating the effects of treatment parameters on either the surface or the near-surface residual stress. No study has evaluated the parametric dependence in residual stress throughout the subsurface layers in pursuit of methods for shaping the residual stress field.

The overall objective of this study was to quantify the influence of elastic prestress on the surface and subsurface residual stress fields, resulting from AWJP of metals. The specific aims were to quantify the depth-dependent contribution of treatment parameters to the residual stress and to identify the optimum treatment conditions for maximizing the surface residual stress and the depth of compressive residual stress resulting from AWJP with prestress.

2. Materials and methods

Three metals were selected for the evaluation including a titanium alloy (Ti6Al4V), spring steel (ASTM 228) and nickel alloy (inconel 718). All three metals were obtained in sheet form having a thickness of 1.5 mm. The mechanical properties of these materials were determined using a tension test and are listed in Table 1. Rectangular specimens were prepared for the AWJP surface treatments with dimensions of 275 mm × 18 mm.

The surface treatments were conducted using an OMAX Model 2652 abrasive waterjet. The nozzle assembly consisted of a 0.36 mm diameter sapphire orifice and a tungsten carbide mixing tube of 0.9 mm internal diameter and 89 mm length. All treatments were conducted with the nozzle oriented perpendicular to the treated surface. A schematic diagram of the peening process is shown in Fig. 1(a) and the treatments were conducted to ensure complete coverage according to the pattern shown in Fig. 1(b). Under the range in treatment conditions explored the

Table 1
Materials and their mechanical properties.

Material	Property					
	Elastic modulus (GPa)	Yield strength (MPa)	Ultimate strength (MPa)	% Elongation	Strength coefficient (MPa)	Strain hardening exponent
Inconel 718	166	950	1650	25.3	2353	0.255
Spring Steel	203	1570	1620	5.1	2320	0.096
Ti6Al4V	111	1016	1080	13.2	1309	0.067

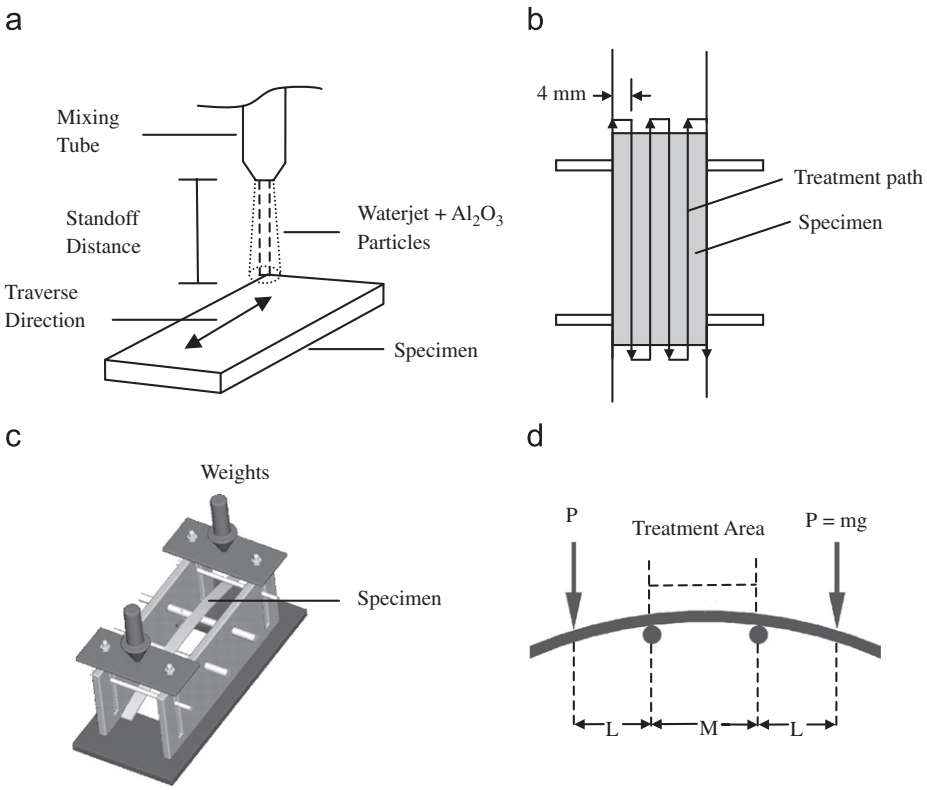

Fig. 1. Details pertaining to the AWJP treatments and the application of prestress: (a) process parameters for treatment and (b) treatment path (c) prestress fixture and (d) prestress loading arrangement (L = 89 mm and M = 83 mm).

diameter of the treatment area is approximately 11 mm, and the corresponding area of jet impingement is $1\times10^{-4}\,m^2$ per unit time. Treating the samples according to the path shown in Fig. 1(b) resulted in approximately 70% overlap between two adjacent passes. A uniform elastic prestress was achieved by placing the specimens in a specially designed fixture to administer 4 point flexure (Fig. 1(c)). Dead weight loads were used to obtain a constant bending moment and a uniform prestress over the region of treatment (Fig. 1(d)). The fixture and dead weights resulted in load control elastic prestress, thereby providing the specimen with the capability to undergo unrestricted elastic recovery during treatment.

Treatments were conducted according to a 9-run, 3-level, 4-factor DOE [15,16]. The parameters involved in the DOE included the jet pressure, abrasive size, elastic limit strain and the elastic prestress. The elastic limit strain was determined by dividing the yield strength of the material by the elastic modulus, whereas the elastic prestress was defined in the DOE as a percentage of the yield strength of the individual materials. Each of the four selected parameters was utilized at three different levels as indicated in Table 2. All of the treatments were conducted using crushed aluminum oxide abrasives with standoff distance and traverse speed of 0.25 m and 2.54 m/min, respectively. A particle flow rate of 0.3 kg/min was used for all treatments, regardless of the particle size, and was achieved by computer control of the machine hardware. These parameters were chosen to maximize the residual stress according to results from a previous study [3]. Three separate 9-run sets of experiments were implemented to achieve a fully crossed DOE and were identified as the low-, medium- and high-level arrays. Parametric conditions for the low-level array are shown in Table 3 and conditions of the medium- and high-level arrays are simple permutations of the low-level array [15,16]. A total of 27 unique surface treatments were performed according to the DOE.

The surface residual stress resulting from AWJP was estimated from the curvature of the specimens and the subsurface distribution was obtained by employing the layer removal method [17–19]. Layer removal was performed using the appropriate etchants for each material. The etching of Ti6Al4V and spring steel was performed using a solution prepared from 20 H_2O:1 H_2O_2:1 HF [20], whereas the inconel specimens were etched using a solution prepared from 42° Baume 9 $FeCl_3$:1 HF. The etching solutions were standardized using test coupons and the etch rate was estimated prior to the experiments to establish appropriate periods of etching and material removed. Furthermore, the untreated side of the specimens was masked using a photoresist to prevent material removal and to ensure that the resulting change in curvature resulted from the treated surface only. Material was removed incrementally and the change in curvature was used to infer the apparent residual stress distribution. In general, the material was removed in increments of 5 μm near the treated surface and in increments of 20 μm further below until there was no change in curvature with further material removal.

Using the estimated curvature from surface profiles, the residual stress was estimated as a function of depth ($\sigma_r(z)$) according to [17,18]

$$\sigma_r(z_1)=\frac{-E}{6(1-\upsilon^2)}\left[(z_0+z_1)^2\frac{d\varphi_x(z_1)}{dz_1}+4(z_0+z_1)\varphi_x(z_1)-\int_{z_1}^{z_0}\varphi_x(z)\,dz\right] \quad (1)$$

where E and υ are Young's modulus and Poisson's ratio of the material, respectively, and z is the depth below the surface. Briefly, a layer of known thickness (t) was removed from the specimen whose surface is initially at a distance z_0 from the neutral axis (Fig. 2). After removal, a new surface with distance z_1 from the neutral axis is obtained. The specimen's curvature was determined before and after material removal using surface profiles obtained using a profilometer. The curvature (φ_x) was plotted against the distance from the neutral axis (z) and a polynomial curve fit was used to obtain a mathematical relationship between the curvature and distance from the neutral axis. The estimated stress was sensitive to the curve fitting technique and a second-order polynomial was found to provide the best fit [19]. A suitable series of such evaluations with depth permitted a quantification of the residual stress distribution according to Eq. (1). The distributions were examined to identify the surface residual stress ($\sigma_{r:s}$), the maximum residual stress ($\sigma_{r:max}$) and the depth of the residual stress (Z_{max}). According to the adopted approach for

Table 2
Surface treatment parameters and the three levels used in the design of experiments.

Level	Parameters			
	Elastic strain, ε_y (m/m)	Pressure, P (MPa)	Prestress, S (% yield strength)	Particle size, G (mesh #)
Low	0.0092 (Ti6Al4V)	103	25	120
Medium	0.0084 (Spring Steel)	172	50	80
High	0.0063 (Inconel)	262	75	54

Table 3
Low-level 9-run design of experiments and treatment responses.

Run	Parameters				Responses			
	Elastic strain	Pressure (MPa)	Prestress (% yield strength)	Grit size (mesh #)	Surface roughness, R_a (μm)	Surface residual stress, $\sigma_{r:s}$ (MPa)	Residual stress depth, Z_{max} (μm)	Stored energy, U (NJ/m^3)
1	0.0092	103	25	120	2.6	470	90	0.4
2	0.0092	172	50	80	9.7	850	310	1.0
3	0.0092	262	75	54	15.6	1450	520	2.4
4	0.0084	262	25	80	10.9	780	330	0.5
5	0.0084	103	50	54	9.4	1040	260	0.9
6	0.0084	172	75	120	4.3	860	110	0.7
7	0.0063	172	25	54	10.4	1500	370	1.9
8	0.0063	262	50	120	4.3	670	200	0.4
9	0.0063	103	75	80	6.0	1390	210	1.9

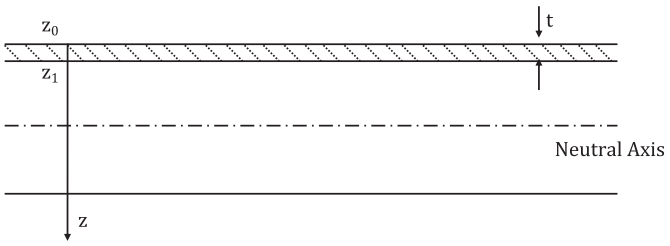

Fig. 2. Schematic diagram of the layer removal method. The variables t, z_0 and z_1 represent the thickness of material removed, initial surface and final surface, respectively. The hatched region represents the layer to be removed by etching.

quantifying the residual stress, the measurement resolution was dependent on the resolution in profile height measurement and its influence on the estimated curvature. The resolution in profile height measurement was 0.1 μm. Using Eq. (1), an error in the radius of curvature of 1 μm resulted in a residual stress measurement error of approximately 200 Pa.

Surface treatments are also often used to induce shape changes in selected targets via the elastic recovery of residual stress. Thus, the elastic energy stored in the surface as a result of AWJP was determined from results of the experiments. Specifically, the subsurface residual stress distribution was plotted with the depth and a quadratic curve used to model the distribution. The specific energy stored (U) was obtained from the subsurface residual stress distribution by integrating it between the surface ($z=0$) and the depth of compressive residual stress (Z_{max}) according to

$$U = \frac{1}{E}\left[\frac{1}{Z_{max}}\int_0^{Z_{max}} \sigma(z)\,dz\right]^2 \quad (2)$$

where E is the elastic modulus of the substrate.

Surface profiles of the treated specimens were obtained using a commercial contact profilometer (Hommel T8000 stylus surface, Hommel America). The profiles were acquired using a skidless contact probe with a 10 μm diameter and a traverse length of 35 mm. The assessment length was chosen according to an error analysis conducted to minimize errors associated with an inadequate length. Three profiles were obtained parallel to the traverse direction at three different locations. The average curvature (φ) and change in curvature ($d\varphi\,dz$) were used in Eq. (1) to estimate the corresponding residual stress. These profiles were also used in measuring the average surface roughness (R_a) of the samples using a cutoff length of 0.8 mm.

An analysis of variance (ANOVA) was conducted with the surface roughness and residual stress measurements to identify contributions from the treatment parameters to the dependent variables. Single parameter linear and quadratic effects were considered in the ANOVA. In addition, an evaluation of the subsurface dependence on the treatment parameters was obtained using the residual stress distributions estimated from layer removal. Non-linear regression models were developed for the dependent variables in terms of the treatment parameters using a commercial statistical package (Statistical Analysis Software (SAS) Version 9.0). In particular, models were developed for the R_a, $\sigma_{r:s}$ and Z_{max}. Parameters with insignificant effects as identified from the ANOVA ($\leqslant 3\%$) were excluded from the models.

3. Results

The average surface roughness (R_a) resulting from AWJP of the three metals for the low-level array is listed in Table 3. Overall, the range in treatment parameters resulted in an R_a from 2.5 to over 15 μm. In general, treatments conducted with large abrasives and high jet pressure resulted in the highest surface roughness, as expected. Note that treatments conducted on the Ti6Al4V had the highest surface roughness, whereas those conducted on spring steel resulted in the lowest. Results from the ANOVA for the R_a are presented in the form of a scree plot in Fig. 3(a). Both the influential and the non-influential factors were identified from the change in slope. It should be noted that the particle size (G) and jet pressure (P) were the most influential parameters; considering the linear and quadratic effects of single treatment parameters, these two parameters combined for nearly 90% of the total variation in surface texture. An empirical model was developed for the R_a and is given by

$$R_a(\mu m) = 2.23 + (960\varepsilon_y) + (3.1\times10^{-2}P) + (1.1\times10^{-3}G) + (1.9\varepsilon_y P) - (9.0\varepsilon_y G) - (2.7\times10^{-4}PG) \quad (3)$$

where ε_y, G and P correspond to the elastic strain, particle size and jet pressure, respectively. A high degree of correlation ($R^2=0.99$) was obtained between the model and experimental responses, with the average error limited to less than 4%. Using Eq. (3) the influence of jet pressure and grit size on the R_a of Ti6Al4V is presented in Fig. 3(b). As evident in this figure, the R_a increased with increasing jet pressure and particle size, with the largest roughness obtained at the maximum pressure (262 MPa) and abrasive size (mesh #54). The parametric response in Fig. 3 suggests that further increase in R_a is possible using larger particles and jet pressure than those used in the present study.

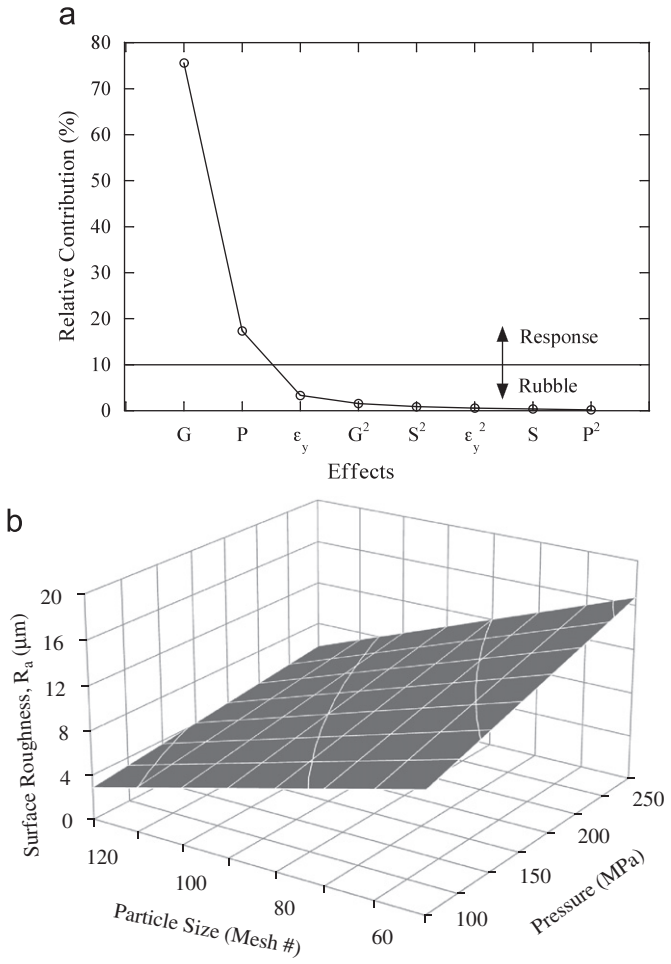

Fig. 3. Surface roughness resulting from the surface treatments: (a) scree plot showing relative contribution of treatment effects on the R_a. (b) influence of grit size and jet pressure on the R_a. The contour plot was developed for treatment of Ti6Al4V ($\varepsilon_y = 0.0092$).

All of the AWJP specimens exhibited concave deflection away from the treated surface, indicating the development of compressive residual stresses and corresponding shape change induced by elastic recovery. As a result of successive layer removal the curvature decreased until the specimens returned to their stress-free state. The variation of curvature with respect to the distance from the neutral axis for a representative spring steel specimen is shown in Fig. 4(a). The corresponding subsurface residual stress distribution is shown in Fig. 4(b). For clarity, the surface residual stress ($\sigma_{r:s}$) and the depth of compressive residual stress (Z_{max}) are highlighted in this figure. Note that the largest residual stress developed at the surface of the specimen, indicating that $\sigma_{r:s} = \sigma_{r:max}$.

Considering results obtained for all three materials, the estimated $\sigma_{r:s}$ ranged from 470 MPa to approximately 2500 MPa. Specific results for specimens of the low-level 9-run array are listed in Table 3. The largest residual stress was achieved in the inconel and was obtained with the highest pressure (262 MPa), abrasive particle size (mesh #54) and prestress (75%). The relative contribution of the treatment parameters on the $\sigma_{r:s}$ is shown in Fig. 5(a). Consistent with the parametric effects on the R_a, the abrasive particle size was the most influential parameter to the surface residual stress. However, the elastic limit strain and the magnitude of prestress were also identified as main effects. Considering the linear and quadratic effects, the abrasive

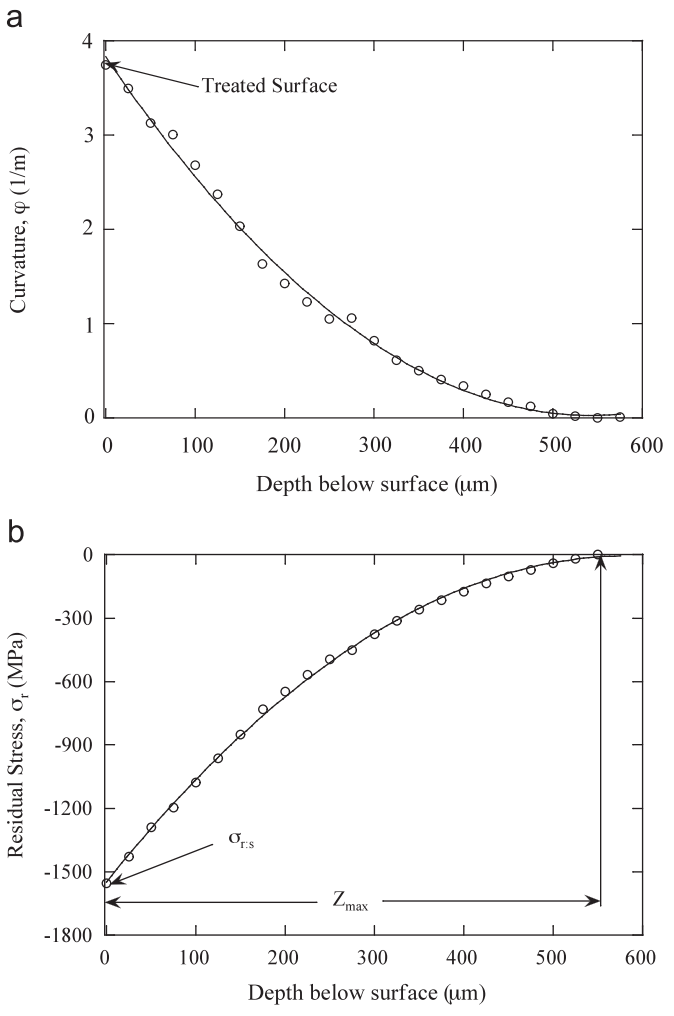

Fig. 4. Subsurface distribution in curvature and residual stress for a representative spring steel specimen treated under an elastic prestress of 75%, treatment pressure of 262 MPa and mesh #54 abrasives: (a) curvature distribution and (b) residual stress distribution.

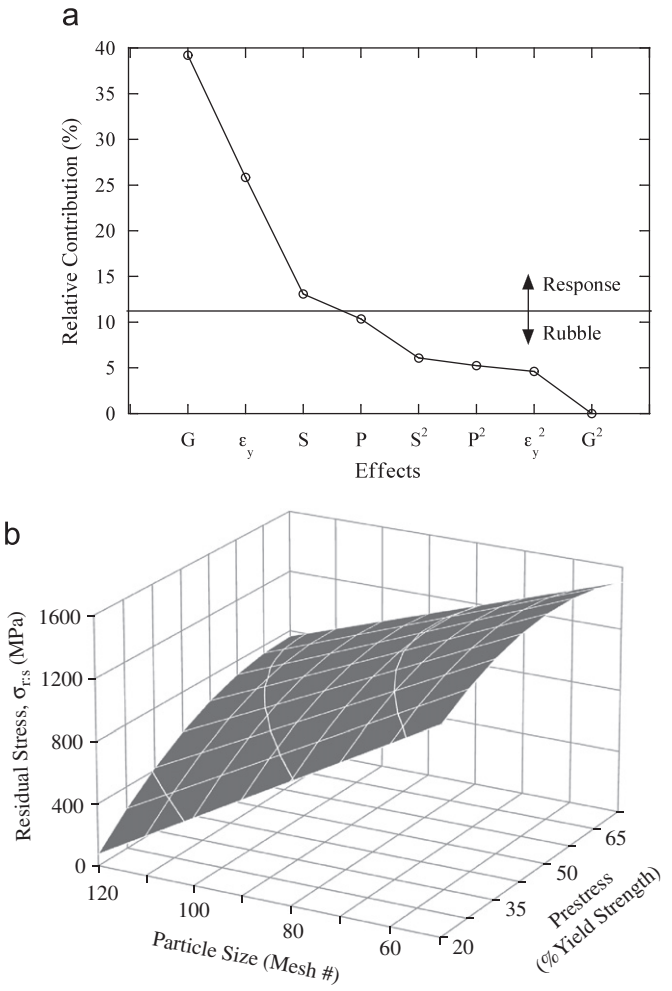

Fig. 5. Residual stress resulting from treatments: (a) scree plot showing relative contributions of treatment effects on the total variation of s:s and (b) influence of grit size and prestress on s:s. The contour plot was developed using a jet pressure of 262 MPa for Ti6Al4V ($\varepsilon_y = 0.0092$).

particle size, elastic limit strain and prestress accounted for nearly 90% of the total variation in $\sigma_{r:s}$. A non-linear regression model was developed to describe the $\sigma_{r:s}$ resulting from AWJP and is given by

$$\begin{aligned}\sigma_{r:s}(\text{MPa}) = {} & 5990 - (1.2\times10^{6}\varepsilon_y) + (3.4P) + (3.1\times10^{3}S) \\ & - (25.4G) - (2.5\times10^{3}S^2) + (4.6\times10^{7}\varepsilon_y^2) + (3.6\times10^{3}G\varepsilon_y) \\ & + (13.8GS) + (2.6\times10^{-2}P^2) + (0.1PG) - (1.3\times10^{5}\varepsilon_y S) \\ & - (2.3\times10^{2}\varepsilon_y P) \end{aligned} \quad (4)$$

The correlation coefficient was 0.96 and a comparison of the residual stress estimated using Eq. (4) with experimental measures resulted in an average error of 9%. Using this empirical relation, the influence of abrasive particle size and elastic prestress on residual stress in Ti6Al4V is presented in Fig. 5(b). As evident from this figure, $\sigma_{r:s}$ increased with increasing prestress and particle size, and a further increase in $\sigma_{r:s}$ may be achieved using larger particles. The potential benefits of using larger prestress will be discussed in the next section.

The depth of compressive residual stress (Z_{max}) was identified from the subsurface residual stress profiles. Considering all three materials, the depth ranged from roughly 80 to nearly 600 μm. Similar to the trend in $\sigma_{r:s}$, the highest depth occurred in treatments conducted with the largest jet pressure, abrasive particle size and prestress. Results of the ANOVA performed with

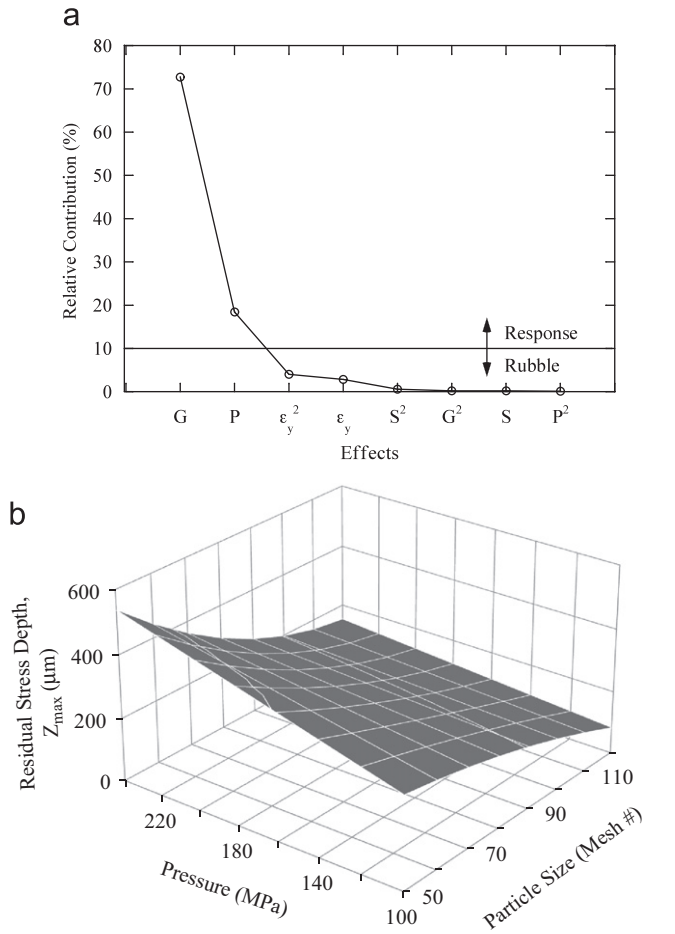

Fig. 6. Depth of residual stress resulting from treatments: (a) scree plot showing relative contributions of treatment effects on the total variation of Z_{max} and (b) the influence of grit size and jet pressure on Z_{max}. The contour plot was developed for Ti6Al4V ($\varepsilon_y = 0.0092$).

the Z_{max} are presented using a scree plot in Fig. 6(a). Consistent with the parametric effects on the R_a, the abrasive particle size and the jet pressure were the most influential parameters to Z_{max}. Considering the linear and quadratic effects, these two parameters combined for 90% of the total variation. A non-linear regression model was developed to describe parametric effects on Z_{max} and is given by

$$\begin{aligned} Z_{max}(\mu m) = {} & 2850 - (6.3 \times 10^5 \varepsilon_y) + (34.9G) + (6.3P) \\ & - (8.7 \times 10^{-2} G^2) + (4.1 \times 10^7 \varepsilon_y^2) - (0.1GP) \\ & + (6.2 \times 10^{-4} G^2 P) - (5.4 \times 10^3 G\varepsilon_y) \\ & - (3.4 \times 10^5 G\varepsilon_y^2) \end{aligned} \quad (5)$$

A correlation coefficient of 0.96 was obtained, and a comparison of Z_{max} estimated according to Eq. (5) with experimental results showed that the average error was less than 9%. Using Eq. (5) the influence of abrasive particle size and jet pressure on Z_{max} for treatment of Ti6Al4V is presented in Fig. 6(b). Note that Z_{max} increased with increasing jet pressure and particle size and a further increase in Z_{max} may be obtained through the use of larger particles and jet pressure than those used in the present study.

The specific energy (U) stored within the near-surface layers of the specimens as a result of AWJP was determined from the subsurface residual stress profiles. The specific energy ranged from 20 KJ/m^3 to nearly 5.5 MJ/m^3. Similar to the trend seen in $\sigma_{r:s}$, the highest specific energy was obtained in treatments conducted with the highest jet pressure, abrasive particle size and prestress. However, results of the ANOVA indicated that there is no single parameter that serves as the primary contributor to the response.

4. Discussion

A systematic study of the parametric effects contributing to the surface texture and residual stress in AWJP with elastic prestress was conducted. Overall results showed that the elastic prestress was one of the primary factors contributing to the $\sigma_{r:s}$ and that the magnitude of residual stress increased with increasing prestress. However, prestress was not influential to the surface roughness. While the Z_{max} can be increased with the application of prestress [11], it was not one of the main effects here with respect to contributions from other parameters. This suggests that the surface stress and depth are not coupled and may be adjusted by the treatment parameters nearly independently.

The treatment process invoked a combination of erosion and localized plastic deformation as a result of particle impact on the substrates. Each of these components of particle/target interaction caused an increase in the R_a. Results from the ANOVA (Fig. 3) indicated that the abrasive particle size and jet pressure were the most influential parameters on R_a, both of which were important to the particle kinetic energy. These results are consistent with previous results for AWJP without elastic prestress [3] and shot peening [4,5]. Previous investigations on shot peening showed that R_a increased with an increase in peening pressure [4] and an increase in shot size [5]. As expected, the applied elastic prestress had minimal effect (Fig. 3(a)) on the surface roughness resulting from AWJP. However, the R_a was dependent on the substrate material, which is attributed to the differences in the erosion resistance of the targets. Material removal in the AWJP treatments is a function of the target's erosion resistance, which is a complex function of the material's elastic modulus, fracture energy per unit area and flow stress [21,22]. It quantifies the ability of the material to resist fracture when it is impacted by an abrasive particle. Out of the three materials used in this study, the Ti6Al4V has the lowest erosion resistance. In turn, the Ti6Al4V underwent the highest degree of material removal, which resulted in the largest R_a. In addition, studies conducted on the surface erosion of metals have shown that the abrasive particle velocity has a profound impact on the resulting material removal [23,24]. In AWJP, the jet pressure controls the velocity of the abrasive particle, and the results of the ANOVA (Fig. 3) showed that pressure is a primary contributor to the resulting R_a. According to Noyan and Cohen [25] there is a relief in the surface residual stress caused by high surface roughness due to the change in orientation of the local free surface plane. As such, the stress relief that occurred in the Ti6Al4V would be expected to exceed that of other materials due to the higher R_a. In shot peening there is a much lower degree of material removal and as a result, the potential for near-surface stress relief is decreased with respect to that in AWJP. Nevertheless, it appears that near-surface embrittlement is far less likely in AWJP than shot peening, a benefit of the erosion process.

The surface and subsurface residual stress fields were obtained for each treated sample using the layer removal technique. Results of the ANOVA for the $\sigma_{r:s}$ indicated that the abrasive particle size, elastic strain and applied elastic prestress were the most influential parameters in the order of contribution (Fig. 5). In shot peening, the magnitude of $\sigma_{r:s}$ increased with increasing shot size [26], elastic prestress [7,8,27] and target material hardness [5]. A related study on shot peening showed that the shot size was the most influential factor to variations in the residual stress [12]. Parametric trends for AWJP in Fig. 5(b) indicate that $\sigma_{r:s}$ increases

with an increase in elastic prestress and suggests that $\sigma_{r:s}$ may be further increased using larger prestress. However, previous studies for AWJP [10,11] and shot peening [27] have indicated that there is a threshold ($\approx$60%) elastic prestress, beyond which there is a minimal change in the magnitude of residual stress. At prestress beyond the threshold the material may reach saturation. Indeed, the inconel specimens treated with the largest prestress and also the largest pressure and grit size exhibited permanent set (i.e. curvature) after the layer removal technique. This implies that elastic recovery of the residual stress and the applied prestress combined to cause yielding of the inconel specimens on the side opposite to that receiving treatment. Neither the Ti6Al4V nor spring steel specimens exhibited permanent set that were treated with the same conditions. Using a thicker sample can mitigate this problem, but it will reduce the sensitivity of the measurement technique used to evaluate the residual stress distribution. Collectively these results highlight that there is a limit to the benefits available from prestress and the limit is material dependent. Materials that have low initial yield strength and have the capacity to undergo significant work hardening may experience gross yielding under excessive prestress.

The influence of treatment parameters on the subsurface residual stress distribution was evaluated as a function of depth using an ANOVA at a series of incremental depths. Specifically, the parametric dependence was quantified in increments of 25 μm beneath the target surface using results of the layer removal evaluation. The relative importance of the treatment parameters as a function of depth is shown in Fig. 7. Over the range of treatment conditions used, the abrasive particle size had the most influence on the subsurface residual stress. Use of larger abrasive particles increases the kinetic energy transferred to the material and the degree of near-surface deformation. This aspect of the treatment dominated the parametric effects beneath the treated surface. These results are consistent with those reported by Freddi et al. [12] on the residual stress at a depth of 25 μm that resulted from shot peening. Interestingly the contribution of particle size increased with depth, whereas the influence of prestress decreased. Indeed, the applied prestress decreased with depth below the surface due to the flexure stress distribution. Release of the prestress resulted in superposition of an elastic component that was a maximum at the surface. Also evident in Fig. 7, the effects of all the variables begin to converge towards an equal contribution (25%) at a depth of approximately 450 μm. The trends in Fig. 7 are expected to be highly dependent on the prestress distribution. Namely, a constant subsurface prestress would result in a larger superposed elastic stress than that obtained using flexure. Further improvement in the subsurface distribution may be possible through the use of alternate prestress conditions. These topics and other potential benefits in AWJP with prestress are reserved for future study.

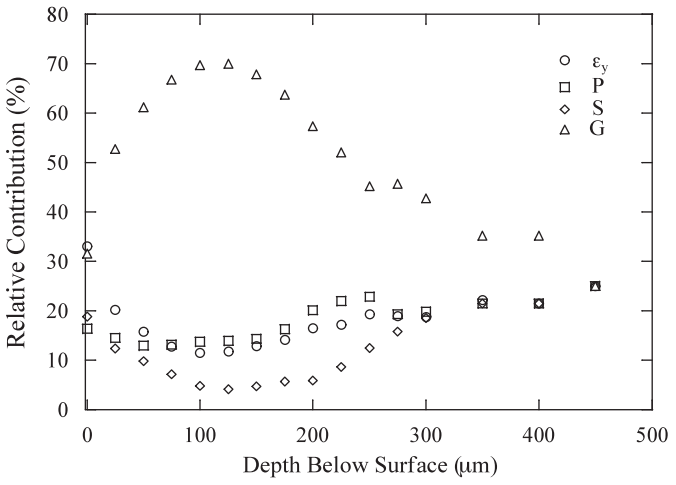

Fig. 7. Relative importance of treatment parameters on the residual stress as a function of depth.

The depth of compressive residual stress (Z_{max}) was determined from the subsurface residual stress profiles. Results of the ANOVA showed that the particle size and jet pressure were the most influential parameters (Fig. 6). Similarly, investigations on shot peening have shown that the depth of compressive residual stress increases with an increase in peening pressure [4] and shot size [26]. A previous study concerning AWJP [11] showed that the depth of compressive residual stress obtained using 75% prestress increased by approximately 50% with respect to the stress-free state. Though elastic prestress was identified as a contributing factor (Fig. 5(a)), it had minimal contribution to the depth of residual stress with respect to the other treatment parameters. Therefore, it appears that the use of a prestress is effective in increasing the depth of compressive residual stress over that achieved in "stress-free" peening, but the parameters influencing the particle kinetic energy are most influential at maximizing the depth of Z_{max}. It is essential to establish conditions that are capable of modifying the desired depth without inducing embrittlement of the surface by excessive work hardening. This aspect of AWJP is reserved for future study, as is the complementary component of evaluation that includes conducting an experimental validation that the increase in residual stress and depth promotes an increase the fatigue strength.

As with all studies, there are some recognized limitations to the investigation that should be addressed. Results were obtained by treating a single specimen under each treatment condition. While one may question the statistical validity of this approach, treatment conditions resulting in the maximum residual stress were used in treating additional specimens, and the variations in the magnitude and depth of residual stress were estimated. The coefficients of variation in the surface residual stress and depth of residual stress were 3% and 5%, respectively. Thus, the variation in the treatment response associated with combined effects of process variation and measurement errors is much smaller than the variations arising from a change in the selected parametric conditions. Also, treatments were performed under a prestress that resulted from load control fixturing. Displacement control fixturing is expected to be more common in a production environment and may result in different parametric trends and residual stress distribution. There may be further benefits to treatments performed using a prestress distribution that utilizes uniaxial tension or a superposition of bending and tension. Future studies should be performed to evaluate these opportunities for optimizing the residual stress field in AWJP or alternative methods of surface treatment with prestress. Despite these limitations, the current study is the first to evaluate the parametric effects of treatment variables on the subsurface residual stress distributions resulting from AWJP with elastic prestress. Further research in this area may lead to the development of a highly viable and effective approach for the surface treatment of metals.

5. Conclusions

An experimental investigation was conducted to evaluate the surface roughness and residual stress field resulting from AWJP of selected metals with elastic prestress. A DOE was implemented and the relative contributions of treatment parameters to the surface texture and residual stress fields were evaluated using an

ANOVA. The results obtained from this study showed the following:

(1) The average surface roughness (R_a) resulting from AWJP ranged from approximately 2.5 μm to nearly 15 μm. The R_a increased with increasing jet pressure and abrasive particle size. There was no influence of prestress on the surface texture.
(2) Compressive residual stresses resulted from all AWJP conditions. The minimum surface residual stress for all treatment conditions was approximately 500 MPa. The magnitude of surface residual stress increased with an increase in abrasive particle size and elastic prestress.
(3) The depth of compressive residual stress ranged from 80 to nearly 600 μm. The depth of compressive residual stress increased with an increase in abrasive particle size and jet pressure, but was not influenced significantly by the applied prestress.
(4) The maximum $\sigma_{r:s}$ was obtained using the largest abrasive particle size and applied elastic prestress. The maximum Z_{max} was obtained using the highest jet pressure and largest abrasive particle size.

Acknowledgement

The authors wish to acknowledge that the investigation was supported in part by an award from National Science Foundation (BES 0521467).

References

[1] D. Arola, M.L. McCain, S. Kunaporn, M. Ramulu, Waterjet and abrasive waterjet treatment of titanium: a comparison of surface texture and residual stress, Wear 249 (10–11) (2002) 943–950.
[2] D. Arola, M.L. McCain, Abrasive waterjet peening: a new method of surface preparation for metal orthopedic implants, Journal of Biomedical Materials Research. Applied Biomaterials 53 (5) (2000) 536–546.
[3] D. Arola, A.E. Alade, W. Weber, Improving fatigue strength of metals using abrasive waterjet peening, Machining Science and Technology 10 (2) (2006) 197–218.
[4] L. Wagner, G. Luetjering, Influence of shot peening on the fatigue behavior of titanium alloys, in: Proceedings of the 1st International Conference on Shot Peening, Paris, France, 14–17 September, 1981, pp. 453–460.
[5] A. Wick, H. Holzapfel, V. Shulze, O. Vohringer, Effects of shot peening parameters on the surface characteristics of differently heat treated AISI 4140, in: Proceedings of the 7th International Conference on Shot Peening, Warsaw, Poland, 28 September–1 October, 1999, pp. 42–53.
[6] G.H. Farrahi, J.L. Lebrun, D. Couratin, Effect of shot peening on residual stress and fatigue life of spring steel, Fatigue and Fracture of Engineering Materials & Structures 18 (2) (1995) 211–220.
[7] J.C. Xu, D.Q. Zhang, B.J. Shen, Fatigue strength and fracture morphology of leaf spring steel after prestressed shot peening, in: Proceedings of the 1st International Conference on Shot Peening, Paris, France, 14–17 September, 1981, pp. 367–371.
[8] C.F. Barrett, R. Todd, Investigation of the effects of elastic prestressing technique on magnitude of compressive residual stress induced by shot peen forming of thick aluminum plates, in: Proceedings of the 2nd International Conf. on Shot Peening, Chicago, USA, 14–17 May., 1984, pp. 15–21.
[9] B. Sadasivam, D. Arola, Application of prestress in abrasive waterjet peening, in: Proceedings of the International Conference on Advances in Materials and Processing Technologies, Las Vegas, NV, USA, July 30–August 3, 2006 (Paper No. NTI2 355).
[10] B. Sadasivam, A. Hizal, D. Arola, Abrasive waterjet peening with elastic prestress: subsurface residual stress distribution, in: Proceedings of the ASME International Mechanical Engineering Congress and Exposition, Seattle, USA, 11–15 November, 2007 (Paper No: IMECE2007–43473).
[11] B. Sadasivam, A. Hizal, D. Arola, An evaluation of abrasive waterjet peening with elastic prestress, ASME Journal of Manufacturing Science and Engineering (2008), in press.
[12] A. Freddi, D. Veschi, M. Bandini, G. Giovani, Design of experiments to investigate residual stresses and fatigue improvement by a surface treatment, Fatigue and Fracture of Engineering Materials & Structures 20 (8) (1997) 1147–1157.
[13] D. Croccolo, L. Cristofolini, M. Bandini, A. Freddi, Fatigue strength of shot-peened nitrided steel: optimization of process parameters by means of design of the experiment, Fatigue and Fracture of Engineering Materials & Structures 25 (7) (2002) 695–707.
[14] P.M. George, N. Pillai, N. Shah, Optimization of shot peening parameters by Taguchi technique, Journal of Materials Processing Technology 153–154 (2004) 925–930.
[15] D. Wheeler, Understanding Industrial Experimentation, second ed., SPC Press Inc., Knoxville, TN, 1990.
[16] D. Wheeler, Tables of Screening Designs, second ed., SPC Press Inc., Knoxville, TN, 1990.
[17] R.G. Treuting, W.T. Read Jr., A mechanical determination of biaxial residual stress in sheet materials, Journal of Applied Physics 22 (2) (1951) 130–134.
[18] J.F. Flavenot, in: Society of Experimental Mechanics, Handbook of Measurement of Residual Stresses, The Fairmont Press Inc., 1996, pp. 35–48.
[19] H.I. Lira, C. Vial, K. Robinson, The ESPI measurement of the residual stress distribution in chemically etched cold-rolled metallic sheets, Measurement Science and Technology 8 (11) (1997) 1250–1257.
[20] K.R. Williams, R.S. Muller, Etch rates for micromachining processing, Journal of Microelectromechanical Systems 5 (4) (1996) 256–269.
[21] Jiyue Zeng, Mechanisms of brittle material erosion associated with high pressure abrasive waterjet processing—a modeling and application study, Ph.D. Dissertation, Department of Mechanical Engineering and Applied Mechanics, University of Rhode Island, 1992.
[22] J. Zeng, K.J. Thomas, R.J. Wallace, Quantitative evaluation of machinability in abrasive waterjet machining, American Society of Mechanical Engineers, Production Engineering Division (Publication) PED 58 (1992) 169–179.
[23] I. Finnie, Erosion of surfaces by solid particles, Wear 3 (2) (1960) 87–103.
[24] M. Hashish, Material properties in abrasive-waterjet machining, Journal of Engineering for Industry, Transactions of the ASME 117 (4) (1995) 575–583.
[25] I.C. Noyan, J.B. Cohen, Residual Stress Measurement by Diffraction and Interpretation, Springer, Berlin, 1987.
[26] A. Niku-Lari, Shot-peening, in: Proceedings of the 1st International Conference on Shot Peening, Paris, France, 14–17 September, 1981, pp. 1–21.
[27] C.C. Osgood, Fatigue Design, second ed., Pergamon Press, Oxford, 1982.